Radar Cross Section Reduction of Microstrip Antenna Using Dual-Band Metamaterial Absorber

Alireza Shater [1] and Davoud Zarifi [2]

[1] School of Electrical and Computer Engineering
University of Tehran, Tehran, Iran
a.shater@ut.ac.ir

[2] School of Electrical and Computer Engineering
University of Kashan, Kashan, Iran
zarifi@kashanu.ac.ir

Abstract ─ This paper deals with the design and experimental verification of a dual-band metamaterial radar absorbing structure for the reduction of radar cross section (RCS) of a microstrip antenna. A Metamaterial Absorber (MMA) is designed to work in X-band with absorption rate near 100%. To demonstrate the effective performance of the proposed structure, its influence on RCS and performance of a microstrip antenna is investigated. According to the numerical and measurement results, one can find that the designed antenna shows dual-band RCS reduction within X-band for wide incident angles, while the radiation characteristics of the antenna are sustained without undesired changes.

Index Terms ─ Dual-band absorber, metamaterial, microstrip antenna, radar absorbing materials, radar cross section.

I. INTRODUCTION

Radar cross section (RCS) reduction has long been an interest of the research community. Stealth technology, which reduces visibility to detection radar, has become a more important and interesting research topic. With the development of the modern stealth technology, RCS reduction has received more attention, especially for the military platforms. For example, a stealth platform should have design features that give it a low RCS. For such low RCS platforms, the antennas which are designed to be effective radiators, have also been the main contributors total RCS. The RCS of a conventional antenna can be very large making it an easy target to pick up on basic radar systems. In fact, if such antenna is placed on a stealthy platform, it will destroy the low RCS properties. Thus, research on RCS reduction for antennas is extremely meaningful.

In recent years, many novel techniques have been proposed to RCS reduction of antennas, such as antenna shaping [1], using radar absorbing materials (RAM) [2-

4], and using cancellation technology [5], [6]. Antenna shaping is widely used to reduce RCS of antenna. With this technique, RCS can be reduced by changing the structures of the original antennas. Another way is the use of RAMs. For in-band frequencies, it is difficult to reduce the RCS using conventional RAMs; because they would severely degrade the performance of the antenna. However, the use of RAMs for the RCS reduction of antenna usually requires a trade-off between radiation characteristics of antennas and RCS reduction effects. Another way to RCS reduction of antennas is the use of Frequency Selective Surface (FSS) radomes [7-11]. In this case, the FSS is transparent to electromagnetic waves in the operating band of antennas, while the signal outside the operating band is reflected. For out-of-band frequencies, FSS can be employed to reduce the RCS of antenna. However, in order to obtain favorable RCS reduction, a complex conformal shape should be designed which increases the complexity, weight and costs.

In 2008, the design of resonant metamaterial absorber (MMA) with near perfect absorptivity has been proposed at microwave band [12]. Later, many efforts have been made on MMA to achieve wide-angle and polarization-insensitive absorption [13-16], multiband absorption [17-19], and broadband absorption [20], [21]. In this contribution, the objective of the present work is to investigate the effect of a dual-band MMA to RCS reduction of microstrip antennas. The proposed antenna exhibits undisturbed radiation performance and dual-band out-of-band RCS reduction for wide incident angles. Also, this approach keeps the advantages of lightweight, low-profile, easy conformal and easy manufacturing nature of the original antenna.

II. DESIGN OF DUAL-BAND MMA STRUCTURE

The layout of the dual-band MMA structure is shown in Fig. 1. The unit cell of this structure constructed

by two metal loops patterned on the FR-4 board. The relative dielectric constant of FR-4 board is 4.35 with a dielectric loss tangent of 0.02. The electromagnetic properties of our proposed structure are characterized using full-wave simulations. Numerical simulations are performed by using periodic boundary condition template and the frequency-domain solver of the CST Microwave Studio (Computer Simulation Technology GmbH, Dermstadt, Germany), which uses a finite element method to determine transmission and reflection coefficients. Unit cell boundary conditions with a tetrahedral mesh were used in the frequency solver, in which case the wave ports were automatically added in the direction of normal incidence to the substrate. The variations of resonant frequency of single-band MMA with parameter l_1 are presented in Fig. 2. It can be clearly seen that, with variation of from 4 to 7 mm, the resonant frequency changes from 12.1 to 5.5 GHz. The presented curve can be used to design arbitrary MMA absorbers. In addition, the proposed dual-band MMA structure can be scaled to achieve desired resonant frequencies.
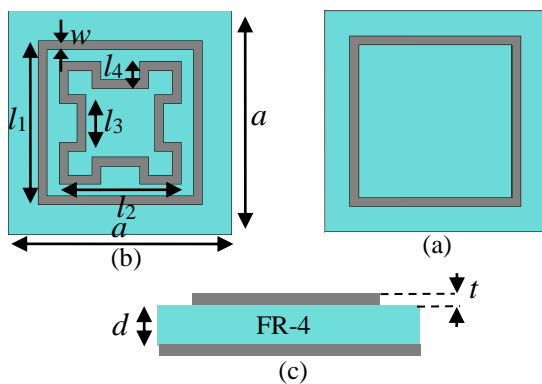

Fig. 1. Unitcell of: (a) single- and (b) dual-band MMA. The dimensions are: $a = 7.5$, $l_1 = 5.5$, $l_2 = 4.1$, $l_3 = 1.9$, $l_4 = 0.9$, $w = 0.3$, and $d = 0.8$.
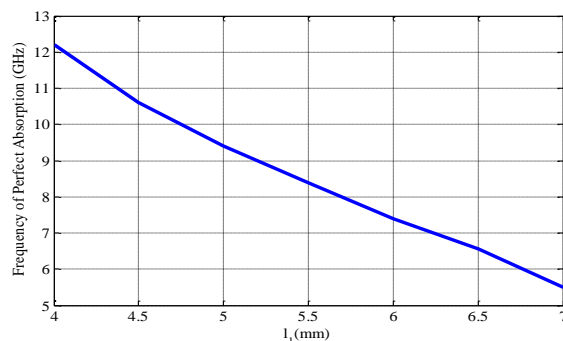

Fig. 2. Variations of resonant frequency of the single-band MMA with parameter l_1.

The designed idea is to adjust the effective and independently by varying the dimensions of loops in

the unit cell so as to match the effective impedance of the structure to free space and achieve a large resonant dissipation in the meantime. Thus, wave transmission and reflection are minimized simultaneously and absorption is maximized. Based on this, the geometry and dimensions of the loops are optimized to achieve two resonance frequencies at the X-band. The numerical simulations are executed in a frequency range of 8–12 GHz. The absorption is calculated as $A(\omega) = 1 - R(\omega) - T(\omega)$, where $R(\omega) = |S_{11}|^2$ and $T(\omega) = |S_{21}|^2$ are the reflectance and the transmittance, respectively. In this case, the metal backing results in $T(\omega) = 0$.

The simulated absorption as a function of frequency is calculated and shown in Fig. 3 for both TE and TM polarizations at various angles of incidence. Observe that for the both TE and TM case, at normal incidence there appear two absorbing peaks that are attributed to two resonant modes. Two perfect absorptivity peaks operating at 8.4 GHz and 10.9 GHz can be obtained; whose absorptivity ratios come up to 99%, and with increasing angle of incidence, the absorption remains quite large. Briefly, the simulation results show that the performance of the absorption of the structure is independent of the angle of incidence and polarization of electromagnetic wave.

The mechanism of the resonance for the MMA structure can be understood by studying the surface current distributions as shown in Fig. 4. Observe that in the first resonance, the majority of induced currents flow on the larger loop. Similarly, in the second frequency band, the majority of induced currents flow on the smaller loop. This shows that the effective frequency bands of this structure are independent and can be simply adjusted. In fact, with poising the length of larger loop and varying of the length of smaller loop, the first frequency band is fixed, while the second one is replaced. The physical mechanism of the absorption of structure is similar to presented discussion in [22], which uses a model based on the destructive and constructive interferences at interfaces.
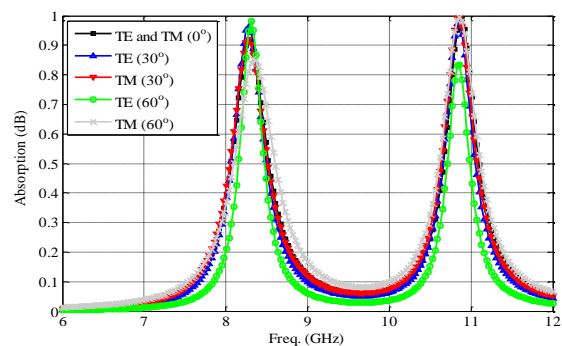

Fig. 3. Absorption of dual-band MMA for various angles of incidence for TE and TM polarizations.
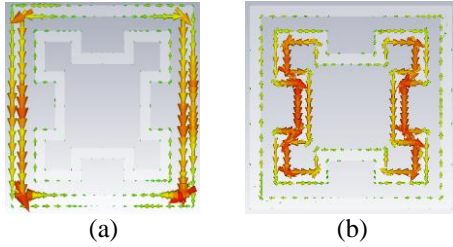
Fig. 4. The surface current distributions on the unit cell of dual-band MMA at the frequencies of: (a) 8.4 GHz and (b) 10.9 GHz.

III. DESIGN OF LOW RCS MICROSTRIP ANTENNA

The geometry of a microstrip patch antenna is shown in Fig. 5. The microstrip patch antenna can be fed by a variety of methods, such as microstrip line feed, coaxial feed, aperture coupled feed, and proximity coupled feed. Here, due to the simplicity, the coaxial or probe feed is used. In the coaxial feed, the input impedance can be adjusted by the probe's location. The optimized location for feed is in $x_f = -2.1$, $y_f = 0$.

The dual-band MMA is applied to the microstrip patch antenna in order to reduce the radar cross section without compromising the performance of antenna. As shown in Fig. 6, this composite structure can act as an antenna as well as an electromagnetic wave absorber.

The simulated S_{11} and radiation pattern of the designed patch antennas with and without MMA are shown in Figs. 7-8. Observe that both of the two microstrip antennas resonated at almost the same frequency of 6.4 GHz with deviation of 50 MHz. Also, according to the results, one can find that the radiation patterns of the proposed antennas in the $\varphi = 0$ and $\varphi = 90$ planes are almost the same. The gain of antenna with MMA approaches 7.15 dB at 6.4 GHz, while the common antenna without MMA has gain of 7.2 dB. The total efficiency of the designed antennas with and without MMA are 52% and 51%, respectively.

The simulated RCS of the microstrip antenna with and without single- and dual-band MMA are calculated and presented in Fig. 9. It can be seen that the frontal RCS of the antenna with dual-band MMA declined from -10 to -30 dBsm and from -8 to -19 dBsm at the frequencies of 8.35 and 11.1 GHz, respectively. Notice that the resonance frequencies of the MMA obtained in the prior sections are valid for a very large structure consisting of many unit cells. Here, due to the physical constraints, the transverse dimensions of the practical MMA should be finite. So, the little difference between the resonance frequencies of the MMA with and without the antenna is due to the finite dimensions of composite structure.

In order to further studies and to illustrate the variation of in-band RCS versus the theta angle, the

RCS of antenna with and without MMA in terms of theta angle are shown in Fig. 10. The results show that the RCSs have been effectively reduced within the angular ranges.
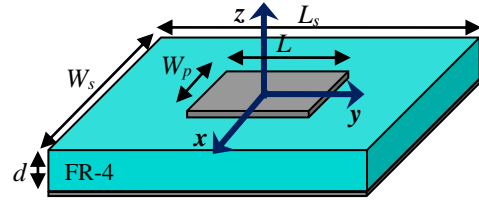

Fig. 5. Microstrip antenna with dimensions of: $L_p = 14.6$ mm, $W_p = 10.6$ mm, $L_s = 52.5$ mm, $W_s = 52.5$ mm, $l_4 = 2.9$ mm, and $d = 0.8$ mm.
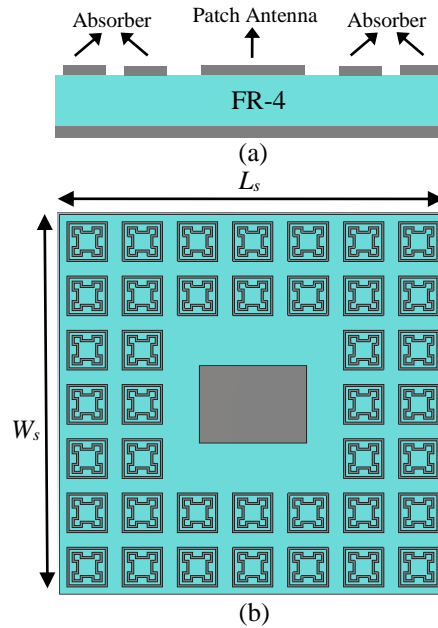

Fig. 6. Configuration of low RCS microstrip antenna. (a) Side view and (b) top view.
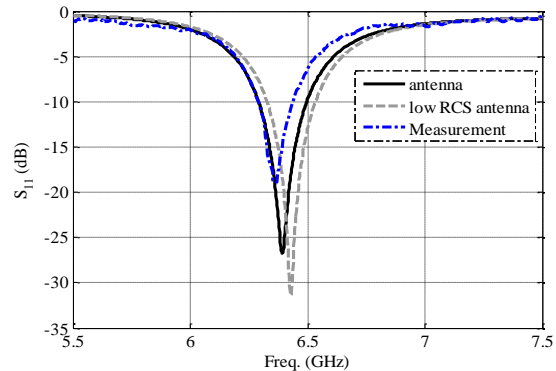

Fig. 7. Simulated reflection coefficients of microstrip antenna with and without MMA.
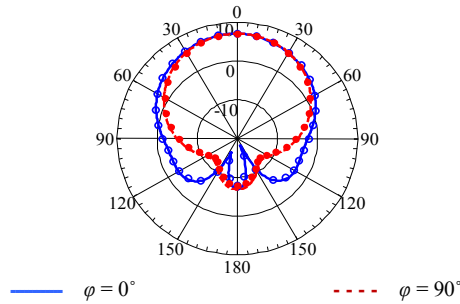
Fig. 8. Comparison of simulated radiation patterns of microstrip antenna with and without MMA at 6.4 GHz. The patterns of low RCS antenna are shown with solid and hollow circles.
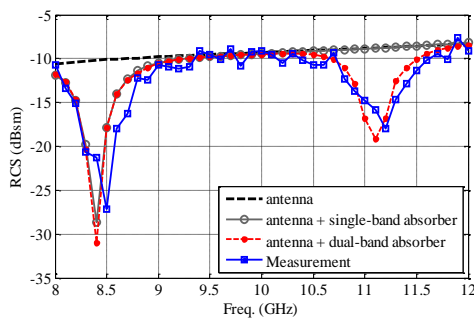

Fig. 9. Comparison of monostatic RCS of microstrip antenna with and without MMA absorber.
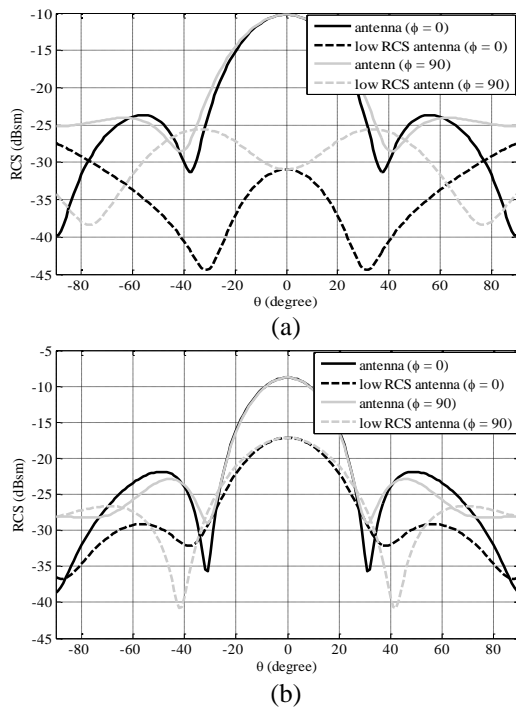

(a)

(b)

Fig. 10. Simulated monostatic RCS of microstrip antenna with and without absorber at under normal incidence at: (a) 8.4 and (b) 11.1 GHz.

IV. FABRICATION AND MEASUREMENT

To validate the design strategies above, the proposed microstrip antenna with MMA absorber is physically fabricated and practically measured. The photograph of fabricated low RCS antenna is shown in Fig. 11.

The input reflection coefficient measured by an HP8720 network analyzer is depicted in Fig. 7 along with the simulated values. Observe that the numerical and experimental reflection coefficients are in very good agreement. The measured center resonance frequency is 6.38 GHz and the measured S_{11} show a small frequency shifts compared with the simulated one. This discrepancy can be attributed to substrate errors and fabrication precision. The monostatic RCS of microstrip antenna with MMA is measured and shown along with the simulated values in Fig. 9. The simulated and measured backward RCS are in very good agreement. Also, the measured and simulated radiation patterns of low RCS antenna at frequency of 6.38 GHz are compared in Fig. 12.
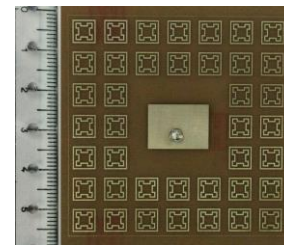

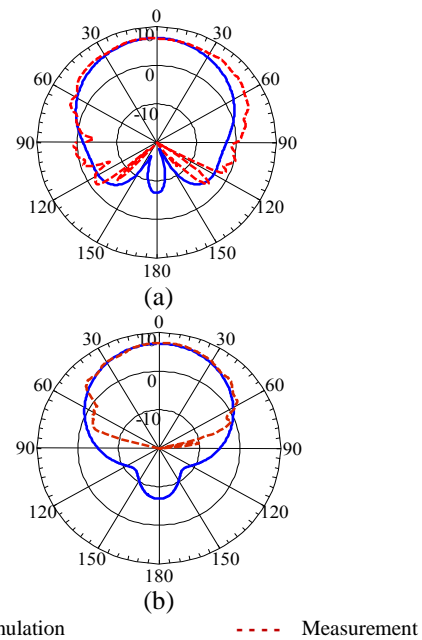Fig. 11. Photograph of fabricated antenna. The dimensions are: $52.5 \times 52.5 \times 0.8$ mm^3.

(a)

(b)

Fig. 12. Comparison of simulated and measured radiation patterns of low RCS microstrip antenna at 6.38 GHz. (a) $\varphi = 0°$ and (b) $\varphi = 90°$.

V. CONCLUSION

Major contribution to the research community discussed in this paper is the RCS reduction of microstrip antenna by using a dual-band MMA. The numerical and experimental results exhibit that it is possible to acquire dual-band RCS reduction by combining microstrip antennas and MMAs. Meanwhile, the performance of microstrip antenna is preserved when the MMA is used. The measured results show that the antenna obtains 20 and 10 dB RCS reduction almost in 8.5 and 11.2 GHz, while its out-band radiation performance is preserved favorably.

REFERENCES

[1] S.-C. Zhao, B.-Z. Wang, and Q.-Q. He, "Broadband radar cross section reduction of a rectangular patch antenna," *Progress In Electromagnetics Research*, vol. 79, pp. 263-275, 2008.

[2] E. F. Knott, J. F. Shaeffer, and M. T. Tuley, *Radar Cross Section*. Raleigh, NC, USA: SciTech, 2004.

[3] K. I. Hopcraft and P. R. Smith, "Geometrical properties of backscattered radiation and their relation to inverse scattering," *J. Opt. Soc. Amer. A*, vol. 6, no. 4, pp. 508-516, 1989.

[4] H. Chen, P. Zhou, L. Chen, and L. Deng, "Study on the properties of surface waves in coated ram layers and monostatic RCS performances of the coated slab," *Progress in Electromagnetics Research M*, vol. 1, pp. 123-135, 2010.

[5] W. Jiang, Y. Liu, S. X. Gong, and T. Hong, "Application of bionics in antenna radar cross section reduction," *IEEE Antennas Wireless Propag. Lett.*, vol. 8, pp. 1275-1278, 2009.

[6] H.-Y. Xu, H. Zhang, K. Lu, and X.-F. Zeng, "A holly-leaf-shaped monopole antenna with low RCS for UWB application," *Progress In Electromagnetics Research*, vol. 117, pp. 35-50, 2011.

[7] H. K. Jang, W. J. Lee, and C. G. Kim, "Design and fabrication of a microstrip patch antenna with a low radar cross section in the X-band," *Smart Mater. Struct.*, vol. 20, p. 015007, 2011.

[8] S. Genovesi, F. Costa, and A. Monorchio, "Low profile array with reduced radar cross section by using frequency selective surfaces," *IEEE Trans. Antennas Propag.*, vol. 60, no. 5, pp. 2327-2335, 2012.

[9] F. Costa, S. Genovesi, and A. Monorchio, "A frequency selective absorbing ground plane for low-RCS microstrip antenna arrays," *Progr. Electromagn. Res.*, vol. 126, pp. 317-332, 2012.

[10] F. Costa and A. Monorchio, "A frequency selective radomes with wideband absorbing properties," *IEEE Transactions on Antennas and Propagation*, vol. 60, no. 6, pp. 2740-2747, 2012.

[11] H. Zhou, S. Qu, B. Lin, and J. Wang, "Filter-antenna consisting of conical FSS radome and monopole antenna," *IEEE Transactions on Antennas and Propagation*, vol. 60, no. 6, pp. 3040-3045, 2012.

[12] N. I. Landy, D. R. Smith, and W. J. Padilla, "A perfect metamaterial absorber," *Phys. Rev. Lett*, vol. 100, p. 207402, 2008.

[13] T. Hu, C. M. Bingham, A. C. Strikwerda, D. Pilon, D. Shrekenhamer, N. I. Landy, K. Fan, X. Zhang, W. J. Padilla, and R. D. Averitt, "Highly-flexible wide angle of incidence terahertz metamaterial absorber," *Phys. Rev. B.*, vol. 78, p. 241103, 2008.

[14] B. Zhu, Z. Wang, C. Huang, Y. Feng, J. Zhao, and T. Jiang, "Polarization insensitive metamaterial absorber with wide incident angle," *Progr. Electromagn. Res.*, vol. 10, no. 1, pp. 231-239, 2010.

[15] F. Dincer, M. Karaaslan, E. Unal, K. Delihacioglu, and C. Sabah, "Design of polarization and incident angle insensitive dual - band metamaterial absorber based on isotropic resonators," *Progr. Electromagn. Res.*, PIER 144, pp. 123-132, 2014.

[16] D. Sood and C. C. Tripathi, "A wideband wide - angle ultra - thin metamaterial microwave absorber," *Progr. Electromagn. Res.*, vol. 44, pp. 39-46, 2015.

[17] Q. Y. Wen, H. W. Zhang, Y. S. Xie, Q. H. Yang, and Y. L. Liu, "Dual band terahertz metamaterial absorber: Design, fabrication, and characterization," *Appl. Phys. Lett.*, vol. 95, p. 241111, 2009.

[18] Y. Liu, Y. Hao, Y. Jia, and S.-X. Gong, "A low RCS dual-frequency microstrip antenna with complementary split-ring resonators," *Progress In Electromagnetics Research*, vol. 146, pp. 125-132, 2014.

[19] G.-D. Wang, J.-F. Chen, X. Hu, Z.-Q. Chen, and M. Liu, "Polarization-insensitive triple-band microwave metamaterial absorber based on rotated square rings," *Progress In Electromagnetics Research*, vol. 145, pp. 175-183, 2014.

[20] J. Lee and S. Lim, "Bandwidth-enhanced and polarisation-insensitive metamaterial absorber using double resonance," *Electron. Lett.*, vol. 47, no. 1, pp. 8-9, 2011.

[21] S. Gu, J. P. Barrett, T. H. Hand, B. I. Popa, and S. A. Cummer, "A broadband low-reflection metamaterial absorber," *J. Appl. Phys.*, vol. 108, p. 064913, 2010.

[22] S. Jamilan, M. N. Azarmanesh, and D. Zarifi, "Design and characterization of a dual-band metamaterial absorber based on destructive interferences," *Progress In Electromagnetics Research C*, vol. 47, pp. 95-101, 2014.

Alireza Shater was born in Iran in 1985. He received the M.Sc. degree from the University of Tehran, Tehran,

Iran, in 2014 in Electrical Engineering. His research interests are inverse problems and metamaterials.

Davoud Zarifi was born in Kashan, Iran, in 1987. He received the Ph.D. degree from the Iran University of Science and Technology, Tehran, Iran, in 2015 in Electrical Engineering. Presently, he is an Assistant Professor in the School of Electrical and Computer Engineering, University of Kashan, Kashan, Iran. His research interests are inverse problems in electro-magnetic, metamaterials and gap waveguide technology.